

COMMISSARIAT A L'ENERGIE ATOMIQUE

FR 8303257

INSTITUT DE RECHERCHE FONDAMENTALE
DEPARTEMENT DE PHYSIQUE GENERALE

SERVICE DE PHYSIQUE THEORIQUE

Q.C.D. ESTIMATES OF HADRONIC CROSS SECTIONS

H. Navelet and R. Peschanski

18. Rencontre de Moriond
La Plagne FRANCE
~~13-19~~ March 1983
CEA-CONF-6684

SPh.T. 83/017

Q.C.D. ESTIMATES OF HADRONIC CROSS SECTIONS

H. Navelet and R. Peschanski
Service de Physique Théorique
CEN - Saclay - 91191 Gif-sur-Yvette Cedex, France

(contributed by H. Navelet)

ABSTRACT

Estimates for hadron-hadron cross-sections are made using the leading log approximation of Q.C.D. The rise of the total inelastic pp cross-sections at high energy is reproduced, thanks to the competition between the small parton-parton interaction and the large multiplicity of gluons predicted by Q.C.D.

RESUME

L'approximation des logarithmes dominants en Q.C.D. est utilisée pour l'estimation de sections efficaces d'interaction hadronique. La montée de la section efficace pp à haute énergie est reliée à la compétition, propre à Q.C.D., entre la faiblesse de l'interaction entre partons et l'abondance de la radiation résultante de gluons.

1. INTRODUCTION

In this work, we will show that gluon radiation induced in hard proton collisions may be responsible for the rise of hadronic cross sections^[1].

Indeed this rise may be obtained by means of small parton-parton differential cross sections weighted by the multiplicity of these partons which is increasing faster than logarithmic. Typical rise of 15 mb between ISR and $p\bar{p}$ collider energy is easily obtained thanks to the increase in the number of gluons radiated by bremsstrahlung^[2].

II. HADRONIC AND PARTONIC CROSS SECTIONS

As usual, in Q.C.D. calculation, we have to separate out the non-perturbative from the perturbative contributions.

i) In a first step, we extract from each incoming hadron, the so-called constituent quark (Valon)^[3] of mass m_q by means of a non-perturbative, Q^2 -independent distribution $\psi_{A \rightarrow \hat{q}_A}(Z)$ which is constrained by

$$\int_0^1 \psi_{A \rightarrow \hat{q}_A}(Z) dZ = N_V \quad (1) \text{ (Conservation of the number of valence quarks } N_V)$$

and

$$\int_0^1 Z \psi_{A \rightarrow \hat{q}_A}(Z) dZ = 1 \quad (2) \text{ (Energy momentum conservation)}$$

ii) One then applies Q.C.D. at the leading log approximation (L.L.A.) in a planar gauge to describe the interaction of these constituents through one gluon exchange. (This excludes the elastic part).

iii) The outgoing partons transform into final hadrons by confinement with an efficiency of 100%. So that, as in e^+e^- total annihilation cross-section, the Non perturbative hadronization does not play any role in the calculus of the total inelastic cross section.

In this scheme, the hadronic cross section is obtained as a function of the partonic cross section as

$$\sigma^{\text{hadronic}}(s) = \int dZ_A \int dZ_B \psi_{A \rightarrow \hat{q}_A}(Z_A) \psi_{B \rightarrow \hat{q}_B}(Z_B) \sigma^{\text{partonic}}(Z_A Z_B s) \quad (3)$$

Our procedure can be represented as a ghost-like diagram^[2] (see fig. 1).

Following D.D.T.^[2], in the L.L.A. and in a planar gauge, partons fluctuations develop from both dressed particles \hat{q}_A and \hat{q}_B . The dominant contributions are the tree diagrams which give rise to generalized ladder diagrams (renormalized vertices and propagators).

The successive virtualities of the partons increase in absolute value from both directions toward the center of the ladder corresponding to the maximum value of the virtuality \hat{t} of the exchanged gluon.

$$\begin{aligned} m_q^2 &<<\dots<< t_A^i \dots << \hat{t} \\ m_q^2 &<<\dots << t_B^j \dots << \hat{t} \end{aligned} \quad (4)$$

These conditions correspond to the strong ordering prescription; t_A^i (resp. t_B^j) represents the absolute value of the virtuality of the i^{th} (j^{th}) cascading parton.

The contribution of these graphs to the partonic cross section is obtained by summation

$$\sigma_{q_A q_B}^{\text{partonic}} = \int_{m_q^2}^{\hat{S}} dt \int_{a,b} \int_{\Delta_{\hat{t}}} dx_a dx_b D_{q_A}^a(x_a, \hat{t}) D_{q_B}^b(x_b, \hat{t}) \times \frac{d\sigma}{dt}(ab \rightarrow ab). \quad (5)$$

where X_a (resp. X_b) is the fraction of the Valon q_A (resp. q_B) momentum, ($0 \leq X_{a,b} \leq 1$), $\hat{S} = Z_A Z_B \hat{S}$ is the C.M. square energy of the Valon-Valon interaction, $D_{q_A}^a(x_a, \hat{t})$ (resp. $D_{q_B}^b(x_b, \hat{t})$) is the probability of finding the parton a (resp. b) of virtuality \hat{t} in a Valon q_A (resp. q_B), $\frac{d\sigma}{dt}(ab \rightarrow ab)$ is the cross section of the one gluon exchange $ab \rightarrow ab$ scattering process. (For large \hat{t} , $\frac{d\sigma}{dt} \propto \frac{1}{\hat{t}^2} \alpha_S^2(\hat{t})$ where $\alpha_S(\hat{t})$ is the running coupling constant $\frac{\alpha_S(\hat{t})}{4\pi} = \frac{1}{b \ln \frac{\hat{t}}{\Lambda}}$, $3b = 11N_c - 2N_f$ where N_c (N_f) is the number of colour (flavor) of the theory).

$\Delta_{\hat{t}}$ is the integration domain described as follow :

i) From kinematics, $\hat{t} < \hat{S}$ where \hat{S} is the C.M. square energy of the two body process $ab \rightarrow ab$ namely $\hat{S} \approx X_a X_b \hat{S}$

ii) From L.L.A., $x_{a,b} \geq m_q^2/\hat{t}$. To prove this second condition, we consider first the cascading of a *time like* parton of virtualness Q^2 down to a Valon.

At step i , $p_T^2 = t_i Z_i (1 - Z_i) - t_{i+1} (1 - Z_i) - m^2 Z_i$ where p_T is the transverse momentum and Z_i is the relative energy of parton $i+1$ with respect to parton

i . The condition that $p_T^2 > 0$ implies $Z_i \geq \frac{t_{i+1}}{t_i}$.

Repeating this argument step by step, we obtain that Z the relative energy of the final Valon is bounded by $Z > m_q^2/Q^2$. At the L.L.A., Gribov Lipatov [4] reciprocity relation holds for *space like* partons which implies $x_{a,b} \geq m_q^2/\hat{t}$. Actually $\Delta_{\hat{t}}$ is simpler in terms of rapidity like variables. See fig. 2.

$$y_{a,b} = \ln \frac{1}{x_{a,b}}, \quad \eta = \ln \frac{\hat{t}}{m_q^2}, \quad \eta_S = \ln \frac{\hat{S}}{m_q^2}.$$

We have 3 domains

$$\begin{aligned} \text{I} \quad & 0 \leq \eta \leq \frac{\eta_S}{3} \quad \Rightarrow \quad 0 \leq y_{a,b} \leq \eta. \\ \text{II} \quad & \frac{\eta_S}{3} \leq \eta \leq \frac{\eta_S}{2} \quad \Rightarrow \quad \{0 \leq y_{a,b} \leq \eta\} \cap \{y_a + y_b \leq \eta_S - \eta\} \\ \text{III} \quad & \frac{\eta_S}{2} \leq \eta \leq \eta_S \quad \Rightarrow \quad y_a + y_b \leq \eta_S - \eta. \end{aligned}$$

III. FORMALISM

a. Valon structure functions

Following Ref. 2, we get the following behavior near $x = 0$ of the gluon and the sea quark structure functions

$$\begin{aligned} x D_q^g(x, \hat{t}) &\propto \frac{I_1(v)}{v}, \\ x D_q^{q_S}(x, \hat{t}) &\propto \frac{I_2(v)}{v^2}, \end{aligned}$$

where $v = \{16 N_c \xi \ln \frac{1}{x}\}^{1/2}$, N_c is the number of colour, I_1 and I_2 are modified Bessel functions which behave as $e^v/\sqrt{2\pi v}$ for large v and

$$\xi = \frac{1}{5} \ln \frac{\ln(\hat{t}/\Lambda^2)}{\ln(\mu^2/\Lambda^2)}, \quad \Lambda = 100 \text{ MeV and } \mu = 150 \text{ MeV in order to get 47% of glue at}$$

$Q^2 = 2.5 \text{ GeV}^2$. Actually L.L.A. applies for small values of x [5] provided

$$1 \ll \ln \frac{1}{x} \leq \ln \frac{\hat{t}}{\Lambda^2}.$$

In our calculation $x_{a,b}$ is always larger than $\frac{m_q^2}{\hat{t}}$ and provided that $\frac{1}{\pi} \alpha_S(m_q^2)$ is small (i.e. $\frac{m_q^2}{\Lambda^2} \gg 1$), the L.L.A. does apply. As we will see later, $\frac{m_q^2}{\Lambda^2}$ turns out to be of the order of 10 ($m_q \approx \frac{1}{3}$ nucleon mass) which yields $\frac{1}{\pi} \alpha_S(m_q^2) \sim 2$.

For valence quarks, the structure function are characterized by a full multiplicity which is finite $\int_0^1 D_{q_A}^V(x) dx = 1$. To make more transparent our calculations, we have factorized the integrals in y_a and y_b in domains II and III by replacing them by a smaller domain II' $y_{a,b} \leq \frac{\eta_S - \eta}{2}$ (Domain I is already factorizable) (see Fig. 2). This will provide us with a lower bound and avoid a specific choice of the valence structure function.

To summarize, this lower bound appears as the integral over \hat{t} of the QCD differential cross section $\frac{d\sigma}{d\hat{t}}$ weighted by the truncated multiplicities $n^{a,b}(\hat{t})$

of the incoming partons a,b. By truncated multiplicity, we mean the integral over x of the structure function running from x_{\min} to 1 where $x_{\min} = m_q^2/\hat{t}$ in domain I and $\sqrt{\tilde{S}/\hat{t}}$ in domain II'. In the case of the valence quark, we just replace the truncated multiplicity by the full multiplicity $n^V(\hat{t}) = 1$. (The integrand is convergent in this case whereas it is severely divergent in the gluon and sea quark case near $x = 0$ as $\frac{1}{x} \exp\{\sqrt{16N_c} \xi \ln \frac{1}{x}\}$. The normalisation of the gluon and sea quark structure functions are fixed by means of the second moment.

All in all

$$\sigma_{q_A q_B}^{\text{part}}(\tilde{S}) \geq \int_{m_q}^{\tilde{S}} \frac{d\hat{t}}{\hat{t}^2} \alpha_S^2(\hat{t}) \left[C_2 \{n^V(\hat{t}) + n^S(\hat{t})\} + n^g(\hat{t}) N_c \right]^2 \quad (6)$$

IV. QUALITATIVE EFFECT

It is possible to understand the origin of the rise of the inelastic hadronic cross-section. For instance let consider the gluon-gluon contribution :

$$\text{In domain I the integrand } I_{gg} \sim \exp\{-\eta + 2\sqrt{16N_c} \xi \eta\} \quad (7)$$

$$\text{whereas in Domain II' } I_{gg} \sim \exp\{-\eta + 2\sqrt{8N_c} \xi (\eta_S - \eta)\} \quad (8)$$

$e^{-\eta} d\eta$ represents the smallness of the partonic interaction ($\frac{d\hat{t}}{\hat{t}^2} \propto e^{-\eta} d\eta$) whereas the term $\exp\{2\sqrt{16N_c} \xi \eta\}$ in the integrand (7) is the enhancement due to the multiplicity of partons. There is a competition between these two factors (the larger the \hat{t} , the smaller $\frac{d\sigma}{d\hat{t}}$ but the larger the multiplicity factor). This is precisely this effect which explains the rise of the partonic cross section.

Indeed, In domain I, $I_{gg} \sim \exp\{-(\sqrt{\eta} - \sqrt{16N_c} \xi)^2\}$ (ξ is a slowly varying function of η) is a gaussian centered at $\eta = 16N_c \xi^2$ which corresponds to $\tilde{S} \lesssim 10^{23} \text{ GeV}^2$ for $m_q \sim M_N/3$.

The logarithmic derivative of this cross section is positive up to this huge value of \tilde{S} and changes sign leading to no violation of Froissart bound. On the contrary in domain II' the logarithmic derivative of the integrand is always negative.

To conclude qualitatively the domain I yields a rise with \tilde{S} corresponding to "semi hard" value of \hat{t} namely $\hat{t} \sim m_q^2 \left\{ \frac{\tilde{S}}{m_q^2} \right\}^{1/3}$. (Typical hard value for large p_T events is $\hat{t} \sim \lambda \tilde{S}$).

V. A QUANTITATIVE ESTIMATE

1) To achieve the calculation, we need to know the non-perturbative part $\psi_{A \rightarrow q_A}(Z_A)$ and $\psi_{B \rightarrow q_B}(Z_B)$ which appear in the formula (3). Fortunately, the partonic cross section depends on $Z_{A,B}$ only through the upper bound $\tilde{S} = Z_A Z_B S$.

Furthermore it turns out that the partonic cross-section is a slowly rising function of energy. This yields the approximate formula for NN cross section

$$\sigma_{NN}^{\text{in}} \approx 9 \sigma^{\text{partonic}} \left(\frac{S}{9}\right) \quad (9)$$

which is nothing but the additive quark model using quark kinematics.

ii) Result.

Our only free parameter is m_q (Λ, μ are given from other analysis^[2])

With $m_q \approx 350 \text{ MeV} \sim \frac{M_N}{3}$, we obtain a rise of the inelastic cross-section of about 15 mb from I.S.R. to $p\bar{p}$ collider energy. To be more specific, we have introduced a new scale Q_T^2 of the order of one GeV^2 ($Q_T^2/\Lambda^2 \geq 10^2$) and cut the integral in \hat{t} into two pieces

$$\int_{\frac{m_q^2}{2}}^{\tilde{S}} d\hat{t} f(\hat{t}) = \int_{\frac{m_q^2}{2}}^{Q_T^2} d\hat{t} f(\hat{t}) + \int_{Q_T^2}^{\tilde{S}} d\hat{t} f(\hat{t})$$

As soon as $\tilde{S} \geq 20 Q_T^2$, the first piece contributes a constant in rough agreement with the data and might correspond to a phenomenological representation of the bare Pomeron contribution whereas the second part which is responsible for the rise of the total cross section is a clean perturbative Q.C.D. effect ($\hat{t} > Q_T^2 \gg \Lambda^2$). For $Q_T^2 = 1.50(\text{GeV})^2$, the constant contribution of the soft region corresponding to the inelastic nucleon nucleon cross section is around 31 mb.

VI. CONCLUSION

i) From this study, we have shown that one gluon exchange in Q.C.D. at the L.L.A. may give a reasonable estimate of the rise of the hadronic cross-section (The higher the constituent quark mass m_q , the smaller the rise).

ii) Multigluon exchange can be incorporated in the non-perturbative "bare Pomeron" contribution.

iii) Radiations of collinear gluons are important in a "semi hard" region ($\frac{\hat{t}}{2} \approx \left(\frac{\tilde{S}}{2}\right)^{1/3}$) where no large p_T events are expected. Jets contributions are recovered at large \hat{t} (Domain III).

In order to study the features of these contributions, we are presently investigating a way to describe the large E_T cross sections from this description.

REFERENCES

- [1] "QCD and the rise of hadronic total cross sections"; G. Cohen-Tannoudji, A. Mantrach, H. Navelet, R. Peschanski, Saclay preprint SPh.T 82/70.
- [2] Yu L. Dokshitzer, D.I. Dyakonov and S.I. Troyan, Physics Reports 58, 270 (1980).
- [3] R.C. Hwa, Proceedings of the Europhysics Study Conference Erice (Italy) 1981, ed. R.T. Van Dewalle.
- [4] V.N. Gribov, L.N. Lipatov, Sov. J. Physics 15 438 and 675 (1972).
- [5] Yu. L. Dokshitzer, JETP 46, 641 (1977).
- [6] M. Haguenaer, UA4 Collaboration presented to the XXI International Conference on High Energy Physics Paris (1982).

FIGURE CAPTIONS

Fig. 1. Ghost diagram exhibiting our ignorance about initial constituent imprisoning (Zone A and B) and colour field trapping in the final state (Zone C).

Fig. 2. The integration domain Δy (shaded area).

Fig. 3. The N-N total inelastic cross section as a function of energy. In dotted line, the constant contribution corresponding to 2 different value of Q_1^2 . Data are from UA4 [6].

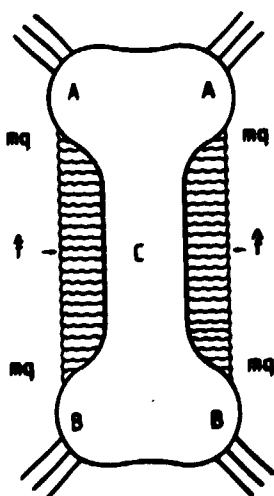


Figure 1.

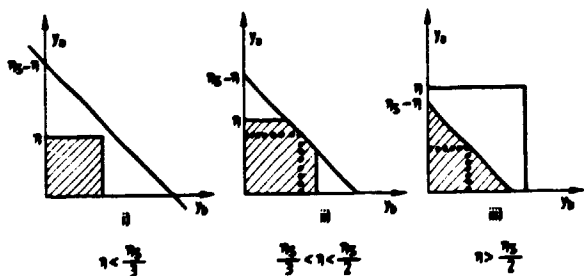


Figure 2.

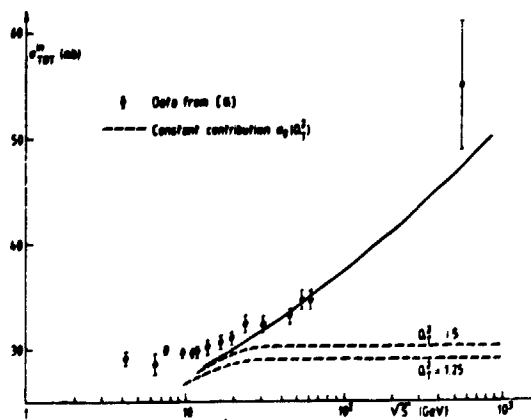


Figure 3.